Journal of Applied Sciences

ISSN 1812-5654

science alert

ANSInet
an open access publisher
http://ansinet.com

Journal of Applied Sciences 8 (23): 4428-4433, 2008
ISSN 1812-5654

Electrical-Transport Studies on $(La_{1-x}Pr_x)_{2/3}Ba_{1/3}MnO_3$ Compounds

[1]H. Abdullah and [2]S.A. Halim
[1]Department of Electric, Electronic and System Engineering,
Faculty of Engineering and Built Environment, Universiti Kebangsaan Malaysia (UKM), Bangi, Malaysia
[2]Department of Physics, Faculty of Science, Universiti Putra Malaysia (UPM), Serdang, Malaysia

Abstract: The magnetic and transport properties of $(La_{1-x}Pr_x)_{2/3}Ba_{1/3}MnO_3$ (x = 0, 0.1677, 0.333, 0.500, 0.677, 0.833, 1.000) compounds, prepared by the solid state reaction have been investigated. The metal-insulator transition (T_p) was determined by using the standard four-point probe resistivity measurement between of 30 and 300 K. With increasing Pr doping, T_p shifted to lower temperatures, which are greater than 300, 270, 250, 226, 202, 186 and 158 K for x = 0, 0.1677, 0.333, 0.500, 0.677, 0.833 and 1.000, respectively. By analyzing the data using several theoretical models, it was concluded that the metallic (ferromagnetic) part of the resistivity (ρ), (below T_P), fits well with the equation $\rho = \rho_0 + \rho_2 T^2$. This indicates that ρ_0 is due to the grain/domain boundary effects. The second term $\sim\rho_2 T^2$ appears to be attributed to electron-electron scattering. In the high temperature range ($T>T_P$) (the paramagnetic insulating regime) adiabatic small polaron models fit well in different temperature regions, thereby indicating that polaron hopping might be responsible for the conduction mechanism. The activation energy (E_a) also increases as the doping concentration increases.

Key words: Metal-insulator transition temperature (T_p), activation energy (E_a), polaron

INTRODUCTION

Transition metal based on mixed oxides exhibit a very rich spectrum of remarkable electric, magnetic and optical properties, tunable by the composition in broad limits. The variety of properties are often due to the different behavior of the 3d electrons, which may be more or less localized, giving rise to intra-atomic correlation effects of different strengths. Rare-earth manganese oxides of the form $Ln_{1-x}A_xMnO_3$ (Ln = rare-earth element, A = alkaline-earth elements) have attracted considerable scientific and technological interest due to their rich physical properties and potential applications. The parent compound of these materials, $LaMnO_3$ $(Mn^{3+}: t_{2g}^3 - e_g^1 : S = 2)$ is an antiferromagnetic insulator characterized by a superexchange coupling between Mn^{3+} sites facilitated by a single e_g electron which is subjected to strong correlation effects. Substitution on La^{3+} site by a divalent alkaline earth ion (A^{2+}) results in a mixed valence Mn^{3+}/Mn^{4+}, where Mn^{4+} lacks e_g electron and hence the itinerant hole associated with the Mn^{4+} ion may hop to Mn^{3+}. However, due to a strong onsite exchange interaction (Hund's rule) with the localized Mn electrons, only hopping between sites with localized parallel spins is favored. This is the essence of the double-exchange model (Zener, 1951) and is believed to explain the physical nature of the interaction and also explains the simultaneous occurrence of ferromagnetism and metallic nature of the material below T_p. The behavior of the electrical resistivity, in the high-temperature ($T>T_P$) regime is also equally complicated as that of the ferromagnetic region. For example, at higher temperatures ($T>T_P$), the formation of polarons and their hopping between different valence states of Mn is not clear. In view of these facts, it is very much essential to investigate the electrical transport both in the ferro magnetic as well as the paramagnetic regions in order to arrive at a comprehensive model (Venkataiah *et al*., 2005). It is well known that change in the grain size has direct consequence on the electronic and magnetotransport properties of a system. In view of this, a systematic investigation on the structural and electrical transport studies of $(La_{1-x}Pr_x)_{2/3}Ba_{1/3}MnO_3$ have been carried and presented in this study.

MATERIALS AND METHODS

This study was conducted in Universiti Putra Malaysia (UPM), Malaysia in 2005. Nominal stoichiometric $(La_{1-x}Pr_x)_{2/3}Ba_{1/3}MnO_3$ (x = 0, 0.1677, 0.333, 0.500, 0.677, 0.833 and 1.000) polycrystalline samples were synthesized by the conventional solid-state reaction

Corresponding Author: Huda Abdullah, Department of Electric, Electronic and System Engineering,
Faculty of Engineering and Built Environment, Universiti Kebangsaan Malaysia (UKM), Bangi, Malaysia
Tel: +603 8921 6310 Fax: +603 8921 6146

method. The starting materials were high purity (99.9%) lanthanum oxide (La_2O_3), praseodymium oxide (Pr_6O_{11}), barium carbonate ($BaCO_3$) and manganese carbonate ($MnCO_3$). All materials were mixed and then heated at 900°C in air for 12 h. After calcinations, the resultant black powders mixture were reground, pelletized and sintered in air at 1300°C for 24 h. Four probe dc electrical resistance measurement were carried out in a closed cycle helium refrigerator in the temperature between of 30 and 300 K. The microstructure was investigated by using a Scanning Electron Microscope from (Leo 1455 VP sem) was used to investigate the electrical properties.

RESULTS AND DISCUSSION

All the $(La_{1-x}Pr_x)_{2/3}Ba_{1/3}MnO_3$ samples show a metal to insulator transition temperature (T_p) below 300 K except for samples x = 0.0. The phase transition (T_p) becomes lower due as Pr constant was increased. A higher T_p for pure $La_{0.67}Ba_{0.33}MnO_3$ obtained at 330 K as reported by Ju *et al.* (1995). Figure 1a-c shows the temperature dependence of resistance for increasing Pr content from x = 0.0 and x = 1. The sample showed semiconducting transport behaviour above T_p and metallic behavior below T_p. The T_p of $(La_{1-x}Pr_x)_{2/3}Ba_{1/3}MnO_3$ decrease linearly with Pr concentration. With increase the Pr doping, T_p shifted to lower temperatures, which are greater than 300, 270, 250, 226, 202, 186 and 158 K for x = 0.000, 0.167, 0.330, 0.500, 0.670, 0.833 and 1.000, respectively (Fig. 1d).

When La was successively substituted by Pr, the nominal ratio of Mn^{3+}/Mn^{4+} and hence the hole density in the system remains unchanged due to the same valence of La and Pr. Due to the smaller size of the Pr ions, the electron bandwidth (b_p) increases and hence the hopping

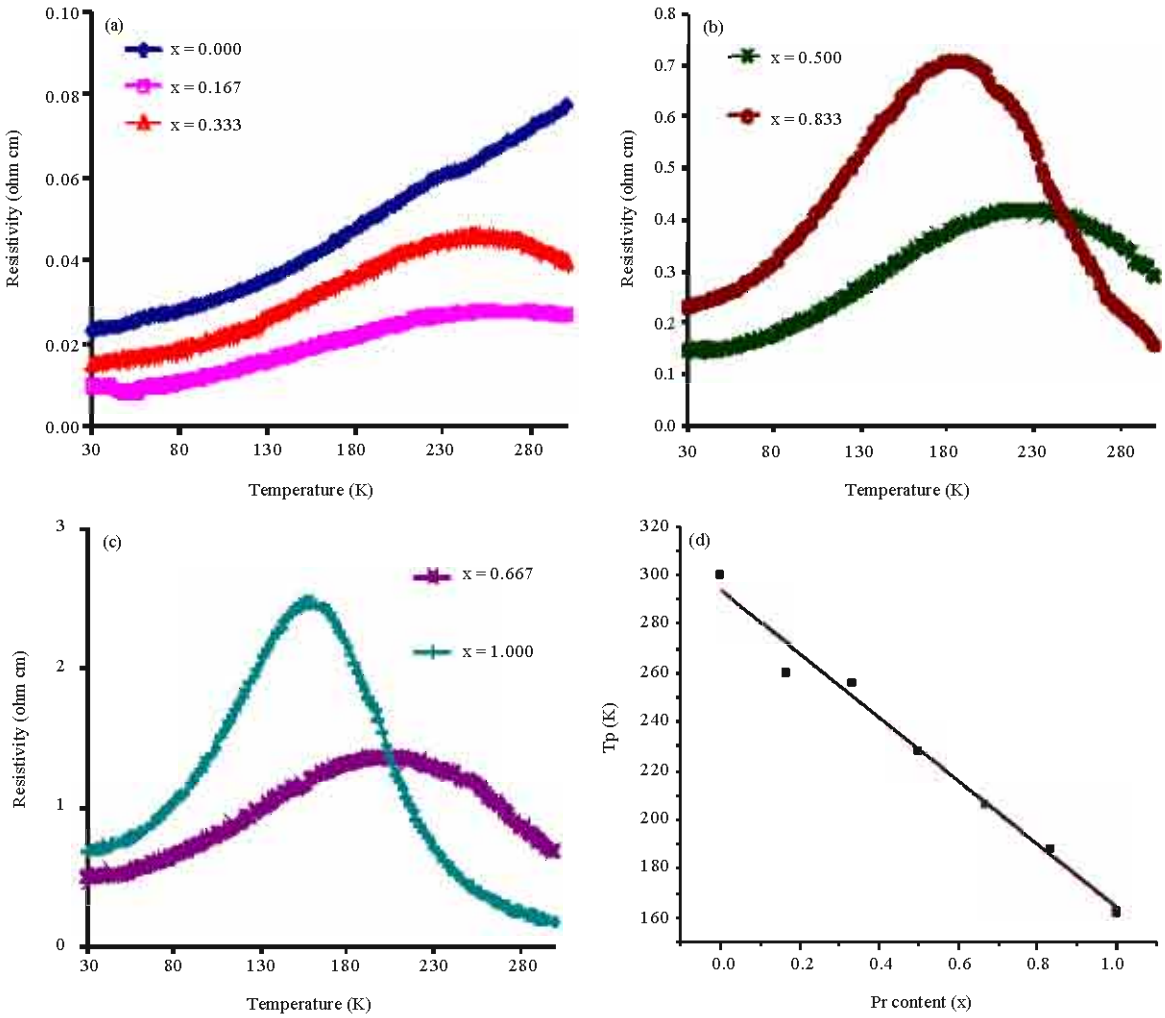

Fig. 1: (a-c): The temperature variation resistance of $(La_{1-x}Pr_x)_{2/3}Ba_{1/3}MnO_3$ samples and (d): T_p of $(La_{1-x}Pr_x)_{2/3}Ba_{1/3}MnO_3$ systems as function of Pr concentration

amplitude for the electrons in the e_g band becomes smaller causing the increment in the resistivity of the samples with the increase in x.

Low-temperature ($T<T_p$) regime: Figure 2 shows the adjusted resistivity versus temperature plot. Below T_p, the electronic conduction mechanism in the ferromagnetic metallic phase is generally understood according to double exchange theory. The Mn^{3+}-O-Mn^{4+} coupling allows conduction through charge transfer from half-filled to empty e_g orbital. In this regime, the metallic behavior of the samples can be explained in terms of electron-magnon scattering of the carriers. In this temperature regime, the resistivity data fit quite well with the following expression:

$$\rho = \rho_0 + \rho_2 T^2 \quad (1)$$

where, the first term ρ_0 corresponds to the resistivity arising due to domain, grain boundary and other temperature independent scattering mechanism. Electron is difficult to cross the boundary due to the disorder of domain and grain boundary. The second term $\rho_2 T^2$ appears as a result of electron - magnon scattering. Thus, the spin scattering cannot be neglected in this regime as the measured data can be best explained by the electron-magnon scattering.

It is noted that the values of both ρ_0 and ρ_2 increase with the increase of x. However, the decrease of temperature independent of ρ_0 is more significant with x compared to that of ρ_2 Table 1. As the doping increases, the size of the domain boundary decreases and ρ_0 becomes larger. The increase of ρ_2 with x is due to the suppression of spin fluctuation.

The microstructure of $(La_{1-x}Pr_x)_{2/3}Ba_{1/3}MnO_3$ with x = 0.000, 0.167, 0.330, 0.500, 0.670, 0.833 and 1.000 are shown in Fig. 3a-g. The micrographs were recorded on the fracture surface of sintered samples. The grain size is in the range of 1 to 3 μm. The grains of samples of x = 0.000, 0.167, 0.330 and 0.500 were observed in round shape, while the others are mixture of round and square shapes. The grain for sample x = 0 is more compact compared to others with average size of ~3 μm and clear grain boundaries. The x = 0.167 to x = 1.000 samples have no clear grain boundary as the grains were too fine. The thickness of grain boundary can be explained by the increment of resistivity. The large pores can be seen in x = 0.500 and 0.833, but the grain size decreases to ~0.8 and ~1 μm, respectively. The grain boundary is clear to see, it was almost 0.33 μm. Figure 3h shows the graph of sample grain size in diameter against the concentration of Pr. The grain size decreases exponentially as the concentration increases. The increment of x from 0.500 to 1.000 show that the change in grain size is not significant. The ionic radius size plays the main role, where the Pr^{3+} ion is smaller than La^{3+}. This indicates that more Pr^{3+} took the place of La^{3+}. In $(La_{1-x}Pr_x)_{1/2}Ba_{1/2}MnO_3$ system, substitution of Pr^{3+} ion for the La^{3+} site in $LaBaMnO_3$ led to grain growth inhibition, lanthanum segregation and second phase formation. Similar observation have been reported by Brzozowski *et al.* (2005), for Nb_2O_5 substituted $BaTiO_3$. The reduction of the size and connectivity between the particles is clearly with different doping concentrations.

High-temperature ($T > T_p$) regime: To explain the electrical conduction just above T_P, i.e., ($T_p<T<\theta_D/2$), (θ_D is the Debye temperature) adiabatic Small Polaron Hopping (SPH) model of Mott has been suggested. This Mott model (Woo-Hwan, 2001) was based on a strong electron-phonon coupling approximation and has been extensively used for explaining the conductivity data of many transition metal oxides. If the charge carriers responsible for conduction are small polarons, the temperature dependence of the DC resisitivity due to hopping process of small polarons predicted theoretically takes the form:

$$\rho = \rho_\alpha T \exp(E\alpha/k_B T) \quad (2)$$

where, E_a is the activation energy and ρ_α is the residual resistivity given by $\rho_\alpha = 2k_B/3ne^2\alpha^2 v$ where, k_B is Boltzmann's constant, e is electron charge, n is number density of charge carriers, a is site-to-site hopping distance and v is longitudinal optical phono frequency (estimated from the relation $h\nu = k_B\theta_D$, where θ_D is the Debye temperature). It has been reported by Hoo-Hwan (2001), the electrical resistivity data, in the temperature region $T > \theta_D/2$ were fitted to the adiabatic small polaron-hopping model represented by the equation, $\rho = \rho_\alpha T \exp(E_\alpha/k_B T)$ and from the best fits, the activation energy values were calculated. Further, θ_D values were also estimated from the plots of ln (ρ/T) versus (1/T) (Fig. 4). It is also clear from Table 2 that the activation energy increases with increase in Pr concentration. This is due to the hole doping in the e_g band, causing the localization of charge carrier to occur and hence increased the energy required to liberate a carrier. Furthermore, E_a values also increases with decrease in the grain size. This behavior may be explained as follows. It is known that with decreasing grain size, the interconnectivity between grains increases, which reduces the possibility of conduction electron to hop to the neighboring site, thereby increasing E_a.

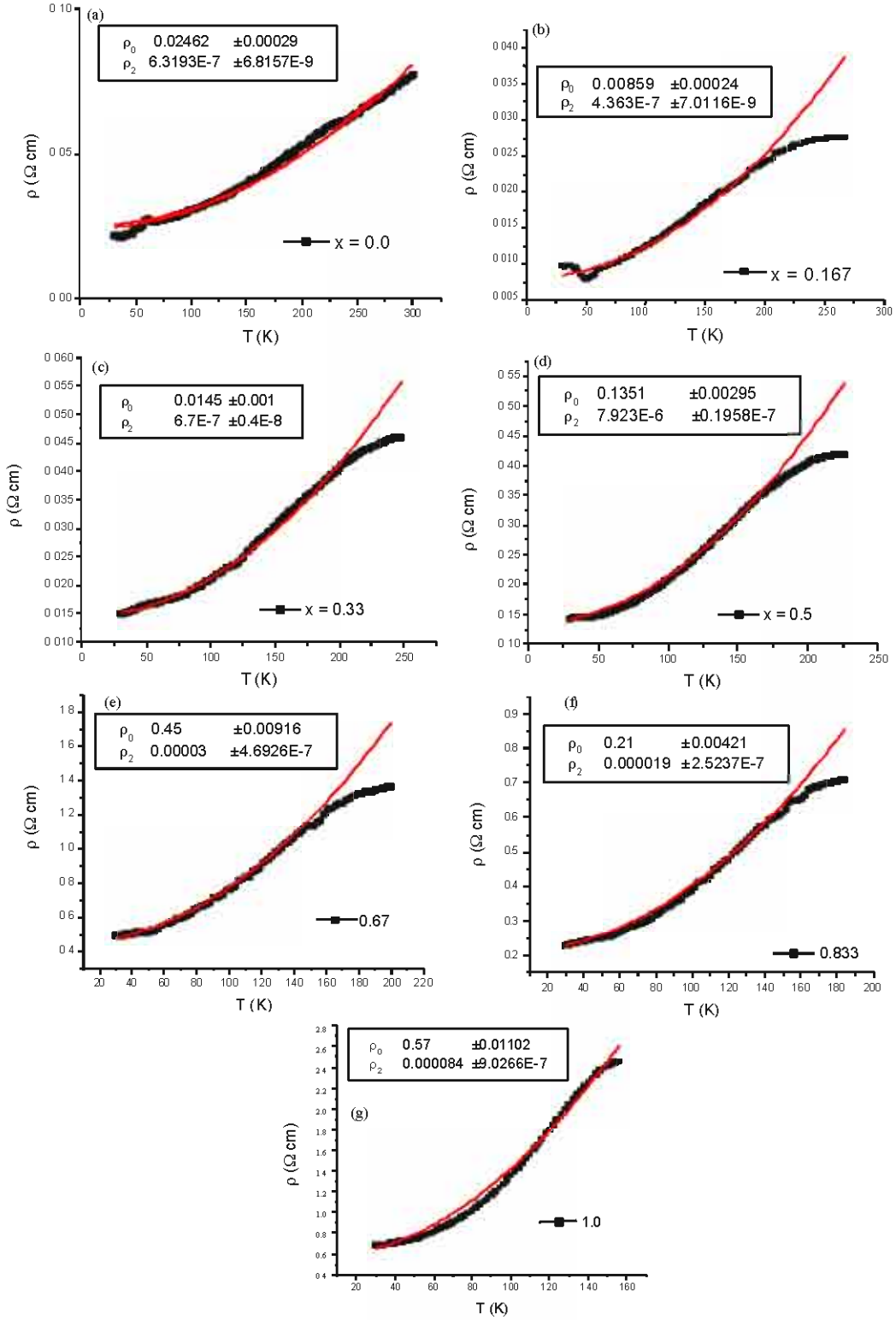

Fig. 2: Adjusted resistivity data showing T^2 dependence for $(La_{1-x}Pr_x)_{2/3}Ba_{1/3}MnO_3$ system below the respective T_p for (a) x = 0, (b) x = 0.167, (c) x = 0.33, (d) x = 0.5, (e) x = 0.67, (f) x = 0.833 and (g) x = 1.0. Solid lines are the best fit to the equation $\rho = \rho_0 + \rho_2 T^2$

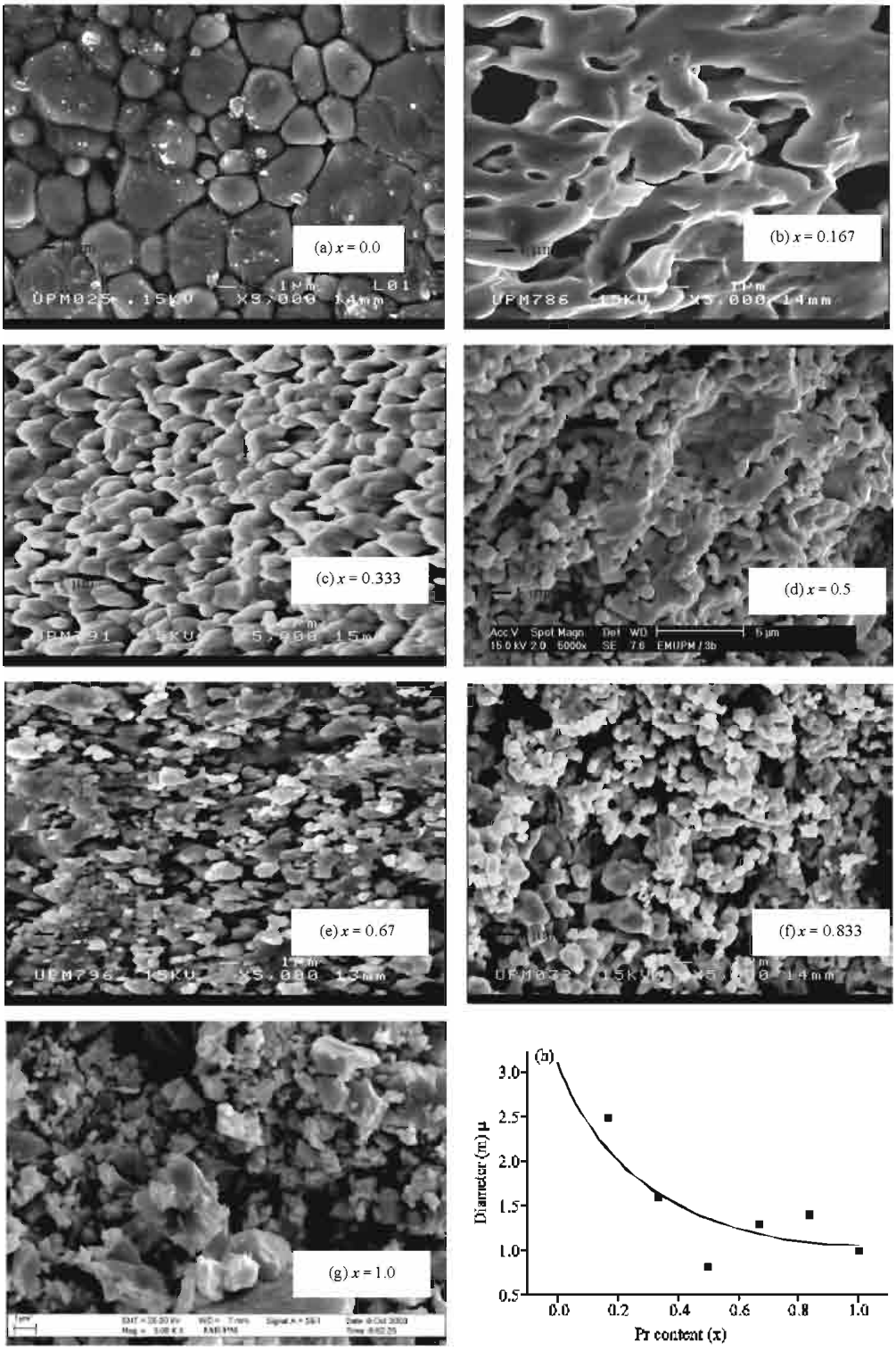

Fig. 3: (a-g) SEM images of the fracture surface of $(La_{1-x}Pr_x)_{2/3}Ba_{1/3}MnO_3$ and (h) grain size of the $(La_{1-x}Pr_x)_{2/3}Ba_{1/3}MnO_3$ system

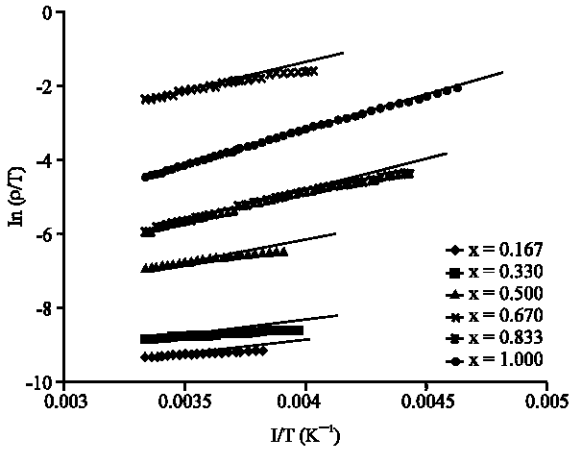

Fig. 4: Plot of ln ρ/T vs. 1/T for $(La_{1-x}Pr_x)_{2/3}Ba_{1/3}MnO_3$

Table 1: The plots of ρ_0 and ρ_2 as function of x

Content (x)	ρ_0 (Ω cm)	ρ_2 (Ω cm K^{-2})
0.000	0.024	6.32×10^{-7}
0.167	0.008	4.30×10^{-7}
0.330	0.015	6.70×10^{-7}
0.500	0.135	7.90×10^{-6}
0.670	0.450	3.70×10^{-5}
0.833	0.210	1.90×10^{-5}
1.000	0.570	8.40×10^{-5}

Table 2: Activation energy, E_a, $\theta_D/2$ and phonon frequency, v (Hz) from resistivity data

x	T_p (K)	E_a (MeV)	$\theta_D/2$ (K)	v (10^{12}Hz)
0.000	>300	-	-	-
0.167	270	30.3	284	5.91
0.330	250	33.5	272	5.67
0.500	226	61.6	252	5.25
0.670	202	84.8	240	5.00
0.833	186	122.0	226	4.71
1.000	158	138.0	200	4.16

Table 2 also shows the phonon frequency against Pr content. It indicates that the frequency of lattice vibration decreases with increasing Pr content. As the concentration of Pr increases, the energy of phonon decreases. This also shows the correlation between T_p and the activation energy (E_a), for conduction in the paramagnetic (PM) phase, where T_p is proportional to the polaron binding energy (E_a). The lattice distortions around the defects favor the localization of the polarons (E_a increases). This becomes apparent in the paramagnetic (PM) phase as an increase of E_a and a decrease of the temperature at which metallic behavior is observed (T_p). We can conclude that in samples without grain boundaries, the T_p is related to the electron-lattice interaction, which is increased by the introduction of chemical defects.

CONCLUSION

The low temperature resistivity signifies the importance of electron-magnon scattering whereas the high temperature transport properties are mainly governed by the small polaron hopping mechanism.

In low temperature resistivity range ($T<T_p$), it can be concluded that the size of the domain boundary decreases and ρ_0 becomes larger, as the doping of Pr increases. The increase of ρ_2 with x is suggested to be due to the suppression of the spin fluctuation. In the high-temperature ($T>T_p$) regime, it is found that the activation energy (E_a) increases with decreasing grain size, as well as increasing Pr doping concentration. This is due to the hole doping in the e_g band, causing localization of charge carriers to occur and hence increases the energy required to liberate a carrier.

ACKNOWLEDGMENTS

The Ministry of Science, Technology and Innovation of Malaysia is gratefully acknowledged for the grant under IRPA vote: 03-02-04-0374-SR0003/07-07 (Fabrication of Magnetic Sensors Head based on Magnetoresistive and Magnetostrictive Thin Films Circuits for Devices Applications) and by UKM-OUP-NBT-26-117/2008 (Group of Nanomaterials Engineering).

REFERENCES

Brzozowski, E. and M.S. Castro, 2005. Grain growth control in nb-doped $BaTiO_3$. J. Mater. Process. Technol., 168: 464-470.

Ju, H.L., J. Gopalakrishnan, J.L. Peng, L. Qi and G.C. Xiong *et al*., 1995. Dependence of giant magnetoresistance on oxygen stoichiometry and magnetization in polycrystalline La0.67Ba0.33MnOz. Phys. Rev. B, 51: 6143-6146.

Venkataiah, G., D.C. Krishna, M. Vithal, S.S. Rao and S.V. Bhat *et al*., 2005. Effect of sintering temperature on electrical transport properties of $La_{0.67}Ca_{0.33}MnO_3$. Physical B, 357: 370-379.

Von Helmolt, R., J. Wecker, B. Holzapfel, L. Schultz and K. Samwer, 1993. Giant negative magnetoresistance in perovskite like $La_{2/3}Ba_{1/3}MnOx$ ferromagnetic films. Phys. Rev. Lett., 71: 2331-2333.

Woo-Hwan, J., 2001. Transport mechanisms in $La_{0.7}Sr_{0.3}FeO_3$: Evidence for small polaron formation. Physical B, 299: 120-123.

Zener, C., 1951. Interaction between the d-shells in the transition metals. II. Ferromagnetic compounds of Manganese with perovskite structure. Phys. Rev., 82: 403-405.